Preliminary Exam Report

Type Ia Supernova Cosmology without Spectroscopic Redshifts

Rebecca Chen

February 28, 2022

1 Introduction

1.1 Cosmological Overview

Cosmology is the study of the origins, history, and evolution of our universe, as well as its components and behavior at the largest scales possible. Our current concordance cosmological model of the universe is the flat-ΛCDM model, where the Λ represents a cosmological constant and CDM is Cold Dark Matter. In this model, the universe's total matter-energy density consists of approximately 70% dark energy, 25% dark matter, and 5% regular baryonic matter. The density parameter for each component is typically defined as a fraction of the total "critical density" ρ_c which is the density required for a flat universe, i.e. $\Omega_i = \rho_i/\rho_c$, where i is Λ for dark energy and M for matter. Despite the successes of the ΛCDM model, we still lack a coherent physical explanation for the fundamental nature of dark energy, the cause of the accelerated expansion of the universe, which remains one of the greatest unresolved scientific questions of our time. Further, recent tensions in cosmology from independent probes point to various discrepancies, either in our treatment of systematic errors, or in the ΛCDM model itself. Improved survey statistics, as well as novel approaches to our distinct cosmological probes, will bring us closer to understanding the source of these tensions.

In order to gain a better understanding and refinement of our best cosmological models, we use a variety of observational probes that are sensitive to different scales, model parameters and periods of cosmic time. One such probe that is particularly sensitive to expansion history is Type Ia Supernovae (SNe Ia), which were used in the discovery of the accelerated expansion of the universe ([1] and [2]). We can characterize dark energy by treating it as a perfect fluid and constraining w, its equation-of-state, defined as $w = P/\rho$ (Pressure/density). If dark energy is a cosmological constant, $w = -1$.

1.2 Type Ia Supernovae

To constrain dark energy, we require a method of measuring distances of far away astrophysical objects. One such method is using standard candles; if we understand the intrinsic luminosity of an object and measure its apparent brightness, we can obtain a measure of its distance from us. Type Ia Supernovae are useful as standard candles both because of our understanding of their consistent explosion mechanisms, as well as their high luminosities, which allows us to observe them out to high redshifts and therefore probe dark energy at different scales.

Supernovae are extremely energetic, transient, astronomical events that can occur at the end of the lifetime of a massive star. This explosion is observed as a gradual brightening and then fading in the sky, and the resulting light curve and information about the change in luminosity over time is home to large amounts of astronomical information. Supernovae are typically classified by their explosion mechanisms as Type Ia (thermonuclear SNe), or core-collapse SNe (Types Ib, Ic, II). In particular, they can be identified by the presence (or lack thereof) of certain spectral features. For instance, Type Ia supernovae show no hydrogen in their spectra, but present a strong Si II line.

In particular, SNe Ia are theorized to form under two models, one of which has single and the other double progenitors. In the single degenerate model, the more massive star in a close binary system evolves into a giant, engulfing the secondary star in gas. The primary star eventually evolves into a white dwarf and the secondary star evolves into a giant. The secondary then accretes mass onto the white dwarf as they inspiral. If the white dwarf's mass reaches the Chandrasekhar limit, the mass at which gravity overcomes electron degeneracy pressure, it explodes as a supernova. In the double degenerate model, two orbiting white dwarfs merge and their combined mass exceeds the Chandrasekhar limit, triggering the SNIa.

SNe Ia are frequently referred to as standard candles due to their consistent peak luminosity (due to the mechanisms that trigger their explosions). Our understanding of the intrinsic luminosity of SNe Ia (absolute peak magnitude ~ -19.5) allows us to obtain a measure of their distance upon measuring their apparent magnitude. SNe Ia are sometimes emphasized as "standardizable candles" due to the fact that in reality their absolute magnitudes are not perfectly uniform, with a dispersion of ~ 0.8 mag at peak in the B band. However, the small variation in peak magnitude can be corrected for using correlations between the peak brightness and different fit properties of the light-curve. After standardization, the scatter can be reduced to $\sim$ 0.01 mag, which corresponds to $\sim$ 5% in distances.

2 SNIa Cosmology

2.1 Hubble Diagram

To appropriately standardize the SN brightnesses and estimate their distances, we must use a light-curve model to fit the light-curve properties. One model used to fit light-curves is the SALT2 model [3, 4], which is parametrized by an overall flux normalization (x_0), a shape-related parameter (x_1, or "stretch") and a color parameter (c). We define the distance modulus μ, which is proportional to the logarithm of the luminosity distance $\mu = 5 \times \log(d_L/10\text{parsec})$ or $\mu = m - M$ (apparent magnitude - absolute magnitude). After fitting light-curve parameters, the distance modulus can be estimated using the Tripp estimator [5, 6]:

$$\mu = m_B + \alpha x_1 - \beta c - M_0 + \delta\mu_{\text{bias}} \qquad (1)$$

where M_0 is the SNIa absolute magnitude, $m_B = -2.5\log(x_0)$, α and β are coefficients parametrizing the relationship between stretch, color, and luminosity, and $\delta\mu_{\text{bias}}$ is the distance bias correction which will be described below.

With the estimated distances, along with redshifts, we can construct a Hubble Diagram (distance vs. redshift). To constrain cosmological parameters, we compare estimated distance moduli with theoretical distance moduli, which are computed with a given cosmological model with parameters C. This difference between observed and theoretical distances is called a Hubble residual ($\Delta\mu$), which can be used in a χ^2 fit to determine the best fit cosmological model parameters. Figure 1 shows the Hubble Diagram from the original [1] result, which provided some of the first evidence for the accelerating expansion of the universe.

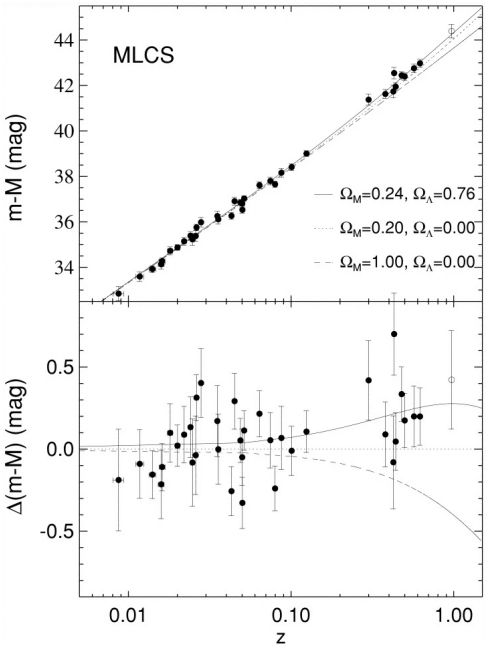

Figure 1: Hubble Diagram from [1]. The top panel plots the distance modulus on the y-axis against redshift on the x-axis. The bottom panel plots the Hubble residuals as a function of redshift. Both panels have theoretical cosmology curves overplotted, showing that a model with non-zero dark energy density provides a better fit to the data.

2.2 Bias corrections and Simulations

As previously mentioned, a distance bias correction is required in order to account for dispersion and our observational magnitude limit. This bias is determined from large simulations which contain detailed models of the observing conditions, telescope efficiency, and selection efficiencies for a given survey. Many modern SNIa analyses utilize the Supernova Analysis software (SNANA, [7]), which forward model SNe Ia with catalog level simulations (i.e. fluxes are computed from image properties, rather than simulating SN light-curves directly onto images). These simulations begin with a source Spectral Energy Distribution (SED), which then has various astrophysical effects applied, such as host galaxy extinction, cosmological dimming, lensing magnification, redshifting, etc. The SED is then integrated across filters and noise is then added based on the instrumental effects, i.e. survey and telescope characteristics such as sky noise, PSF. Lastly, the trigger logic for a detection is implemented, including the selection efficiency of spectroscopic follow-up.

These detailed simulations can be used as inputs to the 'BEAMS with Bias Corrections' (BBC, [8]) method, which marginalizes over classification probabilities to produce a bias-corrected SNIa Hubble Diagram.

2.3 Modern Challenges

While the distance measurement is a crucial part of the SNIa cosmology analysis, there remain two additional important areas of consideration. The first of these is classification of the SN. The SNIa standardizable candle method relies on our ability to accurately determine whether an observed SN is actually a Type Ia or whether it is a core-collapse SN. Historically, SNe have been classified spectroscopically, with spectral features. However, SNe can also be classified photometrically, with fluxes from a discrete number of passbands (filter wavelength ranges). Samples of supernovae that contain exclusively spectroscopically confirmed Type Ia are dubbed "spectroscopic samples" and those that rely on photometric classification methods are dubbed "photometric samples." The second important component is that of redshifts. SNIa analyses have relied on spectroscopic redshifts (spec-z) from either the SN itself or its host-galaxy, which is easier to obtain, as it is not time-limited and can be supplemented from various sources.

With this context, there are three major challenges that SNIa cosmology is facing for future SNIa surveys:

i) measuring redshifts from the supernova or its host galaxy

ii) classifying SNe without spectra

iii) accounting for correlations between the properties of SNe Ia and their host galaxies

2.3.1 Redshifts

To obtain precise measurements of redshifts, SN surveys typically require spectroscopy of either the SN itself or its host galaxy. Large-area surveys such as the Dark Energy Survey (DES, [9]) have relied on spectroscopic host-galaxy follow-up programs, either after the main survey has concluded (and the SN itself has faded), or dynamically as the survey is occurring. Host-galaxy redshifts are typically easier to obtain, as there is not a limited time window while the SN is still present, and spectral resolution is typically better. For instance, DES had a concurrent program called OzDES [10] that measured redshifts during the survey, using the AAOmega spectrograph on AAT, as the 2dF fiber positioner + AAOmega has a similar field-of-view to the Dark Energy Camera (DECam). However, this approach to obtaining redshifts is limited, as even with multi-object targeting, spectroscopy requires large amounts of dedicated telescope time. Further, follow-up spectroscopy introduces the requirement for additional modeling of spectroscopic efficiency for our simulations and bias corrections due to observational biases toward brighter host galaxies. While the follow-up strategy has been feasible thus far for our current photometric surveys, future surveys such as the Vera Rubin Observatory Legacy Survey of Space and Time (LSST), which will observe on the order of millions of SNe, will not physically be able to obtain spectroscopy for all SNe or their host galaxies. Current projections for the spectroscopic follow-up of transients from LSST (TiDES; the Time-Domain Extragalactic Survey [11]) predict that we will be able to obtain spectra for up to 30,000 live transients and measure redshifts for up to 50,000 host galaxies. While this is an order of magnitude larger than our current SNIa samples ($\sim$ 1700), it is still a small fraction of the total predicted $\sim$ 2.4 million SNe (that pass light-curve quality cuts) that LSST will observe.

An alternative to this reliance on spectroscopic redshifts is photometric redshifts (photo-z), which uses the photometry from a relatively small number of filters to estimate the redshift. These redshifts are typically much less accurate and precise, as the inference is from a discrete amount of flux information, rather than a continuum. Despite the ubiquity of photometric redshift estimates in other cosmological analyses such as weak lensing, there have thus far been limited studies on using photo-z in a cosmological study with SNe Ia. Studies such as [12] found that using photo-zs derived from the SN light-curve itself with real SDSS data resulted in pathologies that propagated to biases in the distances and therefore the measurement of cosmological parameters.

2.3.2 Classification

SN classification has also historically relied heavily on spectroscopy. Photometric classification has been a large area of focus for many years, with a number of approaches, algorithms, and methods being tested. One such effort was the Photometric LSST Astronomical Time-series Classification Challenge (PLAsTiCC). The top performing light-curve classifiers in the challenge achieved 95% levels of purity by training on a subset of the data. SuperNNova (SNN), a neural net classifier trained on simulations that use PLAsTiCC models of SNe SEDs, has a predicted efficiency from DES simulations of 97.7-99.5%.

Another approach to photometric classification is to make use of host-galaxy information to avoid problems with poor Signal-to-Noise (SNR) or lack of sufficient observations in the SN light-curve. One such study [13] found that galaxy morphology provides the most discriminating information for determining a SNIa classification probability. Galaxy information is related to SN type, as the SN explosion method/progenitor model is also related to galaxy

evolution and type. For instance, core-collapse SNe have massive ($> 8M_{\odot}$) star progenitors, which is consistent with observations that they explode almost exclusively in gas rich, star forming galaxies such as spiral galaxies. In contrast, SNe Ia have white dwarf progenitors and therefore appear in a variety of host-galaxy types.

2.3.3 Host galaxy-SN correlations

As SNIa samples typically have diverse host-galaxy types, the issue of preferentially targeting brighter galaxies is particularly problematic because there have been observed correlations between the host-galaxy properties and the luminosity of the SNe. Examples of global host-galaxy properties are host-galaxy mass, metallicity and morphological type. These correlations are not well understood and are the subject of ongoing efforts to implement better bias corrections and modeling. Accounting for these correlations appropriately is particularly important, as the measurement of w is based on a relative measurement between distances of SNe at high- and low-redshift, and a redshift dependent selection of galaxy type may cause a significant systematic in measurements of w. One such example of these correlations is the so-called "mass step," which is defined as the difference in intrinsic luminosity after correction between low and high mass galaxies. The "mass step" has historically been accounted for with an additional empirical correction to the distance modulus.

3 My Contributions

Given the modern challenges posed above, we will require new methods of working with large photometric SN samples. In my paper Chen et al. (2022) we investigate a solution to these problems by exploiting SNe located in Luminous Red Galaxies (LRGs), which are a well known homogeneous population consisting of so called "red and dead" elliptical galaxies. LRGs are expected to contain very low rates of core-collapse SNe, as their progenitors are massive and largely present in active star forming galaxies such as spiral galaxies. Secondly, LRG spectra contain a prominent 4000 Å break due to the absorption of metals in stellar atmospheres which enables very precise and accurate photo-z estimates. These galaxies have been used extensively in large-scale structure and weak lensing studies. The photo-z bias of these galaxies can be further improved with the use of red galaxies selected using the redMaGiC algorithm described in [14], which self-trains the color and luminosity cuts required to achieve a desired comoving density and applies a photo-z afterburner to further reduce biases. Lastly, limiting the host-galaxy type allows for a more consistent sample across redshifts that is less sensitive to complicated correlations between SN light curve properties and host-galaxy properties.

3.1 Data (Dark Energy Survey)

I have been conducting research as an active member of the Dark Energy Survey Supernova Working Group. The DES Supernova program (DES-SN) ran for 5 seasons observing with the Dark Energy Camera on the 4 meter Blanco telescope at the Cerro Tololo Inter-American Observatory in Chile. These observations were made in the *griz* filters for 10 3 sq-deg fields at a cadence of 7 days. DES-SN previously published results using the 3-year spectroscopic sample, which contained about 200 spectroscopically confirmed SNe Ia with host-galaxy spectroscopic redshifts. Current efforts are centered around the 5-year photometric sample (DES 5YR sample), which will contain about 1600 photometrically classified SNe Ia with spectroscopic redshifts as well. In my work, I use the DES 5YR sample without any classification applied.

We first restrict our SN sample to those with redMaGiC host galaxies by matching the SN host-galaxy coordinates to the redMaGiC catalog. We find that after light-curve quality cuts 125 SNe, approximately 6% of the $\sim$ 1600 SNe in the 5YR sample, have redMaGiC host galaxies.

To quantify the performance of the photometric redshifts, we define the photo-z bias $\overline{\Delta z}$ as the median of offsets $\Delta z = z_{\rm spec} - z_{\rm redmagic}$, and the photo-$z$ scatter $\sigma_{\Delta z/(1+z)}$ using the robust standard deviation, $1.4826 \times$ MAD, where MAD is the median absolute deviation $\mid \Delta z - \overline{\Delta z} \mid /(1 + z_{\rm spec})$. In Figure 2, I illustrate the performance of the redMaGiC photo-z compared to the spec-z for both the full redMaGiC galaxy sample, as well as the subset that host SNe. We find that the distribution of redshifts and z band magnitudes are similar between the full sample and subsample, with a redshift range of [0.05, 0.95].

3.2 Simulations

To understand the biases that could result due to using photo-z, we use SNANA catalog level simulations to validate our results and analyze alongside the real data. We also use these simulations to generate large samples for determining bias corrections to correct for known selection effects.

We generate realistic Ia light-curves using the SNANA software and build on the simulation inputs from [15] to replicate the DES 5YR photometric sample. The first modification we make is to fit the underlying distributions of SALT2 light-curve parameters c and x_1 as a function of host-

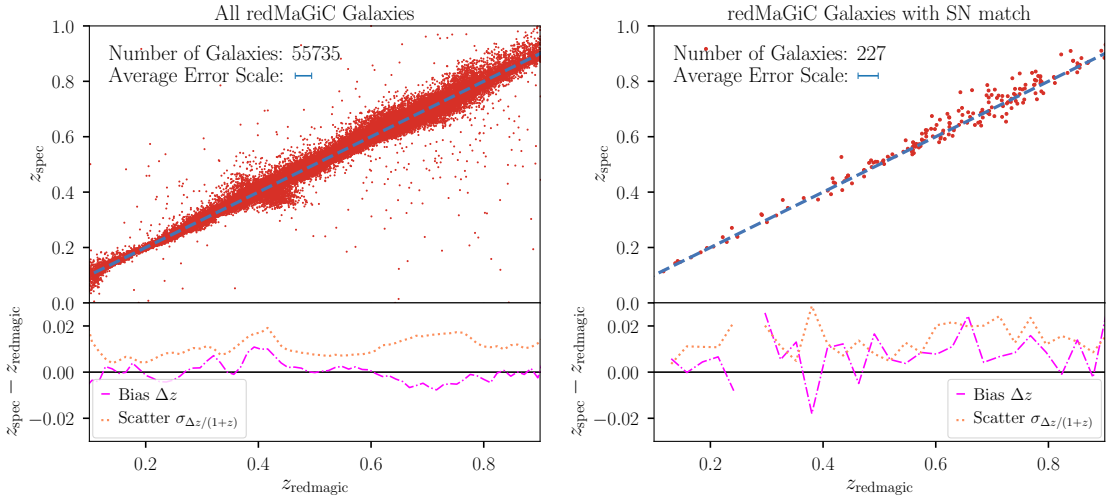

Figure 2: **Top Left:** Photometric redshifts vs. spectroscopic redshifts of redMaGiC galaxies. The dashed line has a slope of 1 for visual comparison. **Bottom Left:** Bias (binned $\overline{\Delta z}$) in dash-dotted pink and scatter in dotted yellow for redMaGiC photo-z. Only galaxies with spectroscopic redshift are included in the bias and scatter calculation. **Right:** Same as left, but for the subset of redMaGiC galaxies with a SN match.

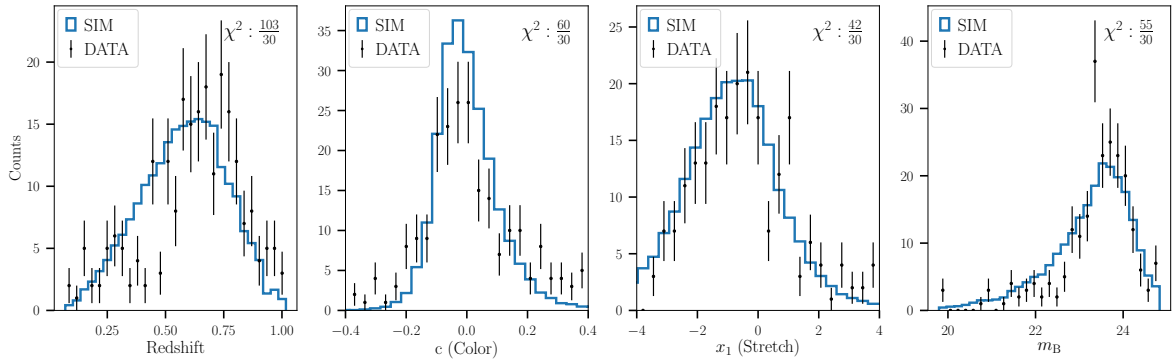

Figure 3: Distributions of redshift (**left**) and light-curve parameters: c (**middle left**), x_1 (**middle right**), m_B (**right**) for data and simulations. The data are represented by the black points, while simulations are represented in blue histogram. Simulation histograms are normalized to the data. The reduced χ^2 value is reported for each parameter.

galaxy stellar mass implemented in [16]. This is necessary to accurately reproduce our observations. We find that the redMaGiC population parameters differ from the DES 3YR spectroscopic sample; in particular, the mean stretch (x_1) value is lower for the redMaGiC subsample, which is consistent with findings from previous studies that find correlations between higher mass galaxies and lower specific star formation rates (sSFR). We also modify the host-galaxy library to mimic the selection of the redMaGiC galaxies. We select only passive galaxies based on the measured log(sSFR) (log(sSFR) < -11.5), apply a cut on the r band magnitude ($m_r < 23.3$) and a cut on the host-galaxy mass (logMass > 10.5).

To accurately characterize the effect of using photo-z, we include a photo-z for each galaxy in the host-galaxy library based on the bias and scatter in the true redMaGiC catalog. For each galaxy in the baseline library, we find its closest match in redshift to the redMaGiC catalog, evaluate the bias $z_{\rm redMaGiC} - z_{\rm spec}$, and add the bias to the true host-galaxy redshift value to determine the photo-z. These photo-z are then propagated into the simulated data.

To validate that our simulations accurately reproduce the data, we compare the distributions for redshift and light-curve parameters as shown in Figure 3. We find good general agreement between the sims and data, with reduced χ^2 values comparable to the current state-of-the-art sims from [15].

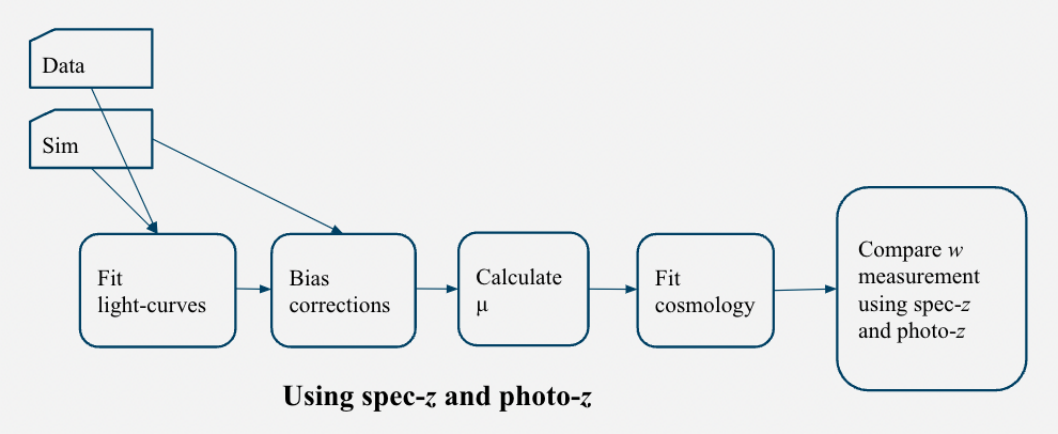

Figure 4: Method Overview

3.3 Main Results

3.3.1 Core-collapse Contamination

To evaluate the claim that redMaGiC galaxies contain very low rates of core-collapse SNe, we consider the classification probabilities for the DES 5YR sample as determined by SuperNNova (SNN, [17]), a photometric neural net classifier. The classifier outputs a probability ranging from 0 to 1.0, with 0 being not-likely Ia. Of the subsample of 125 SNe in redMaGiC galaxies, 4 are classified by SNN as unlikely-Ia (defined by probability of being Ia of < 0.5, $\sim 3\%$ of the sample). For comparison, we look at the classification probabilities for the DES 5YR spectroscopically confirmed SNIa sample, which serves as a "truth" set of SNe Ia. Of the 401 "true" SNIa, 3 are classified by SNN as unlikely-Ia ($\sim 1\%$). We examine the 4 redMaGiC SNe classified as unlikely-Ia; one is a spectroscopically confirmed SNIa, and one is classified as Ia by the baseline SNN from [18]. Another SNN model trained on different templates (J17) classifies two as Ia. We note that photometric classifiers have associated uncertainties and can be affected by errors in the detection and image subtraction process. We confirm the claim that redMaGiC galaxies contain very low rates of core-collapse SNe.

3.3.2 Hubble Diagrams and Cosmological Parameters

To evaluate the potential cosmological biases that could arise as a result of using photometric redshifts, we follow the analysis process detailed in Section 2 and measure cosmological parameters using spectroscopic redshifts and photometric redshifts. We then compare the resulting ws between the two (defined as $\Delta w = w_{\rm spec} - w_{\rm phot}$). This method is also overviewed in Figure 4.

In Figure 5 we show the resulting Hubble Diagram for the simulations. We also consider the Hubble scatter (the scatter of the Hubble residuals), defined with a robust measure of the standard deviation (1.48× MAD) and find that it is consistent to ~ 0.1 mag between the photo-z and spec-z case (0.201 and 0.193 mag respectively). We average Δw obtained over 150 statistically independent simulation instances and find $\Delta w = -0.0011 \pm 0.0020$ with standard deviation 0.0249.

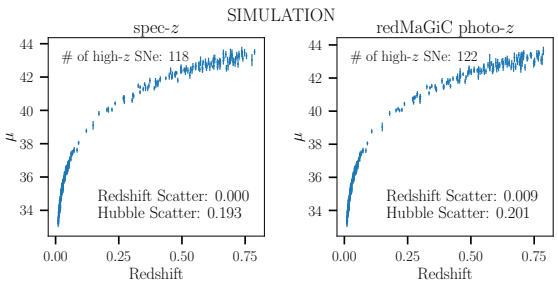

Figure 5: Hubble diagram from analyzing simulation for: spec-z from host galaxy (**left**), redMaGiC photo-zs from the host galaxy (**right**). The number of high-z SNe is shown on each panel, as well as the redshift scatter and Hubble scatter.

We apply the same methods on the data and obtain the Hubble Diagrams shown in Figure 6. Similarly to the simulations, we find the Hubble scatter is consistent to ~ 0.1 mag between the photo-z and spec-z case (0.193 and 0.196 mag respectively). When using redMaGiC photo-z, we obtain $\Delta w = 0.0049$, which is consistent with expectations from simulations and considerably subdominant to the overall data w uncertainty using spec-z (0.0432). This result is an exiting and promising indication that using redMaGiC photo-z in place of spectroscopic redshifts for SNIa cosmology is feasible and that the resulting systematic uncertainties are subdominant to our overall w uncertainty.

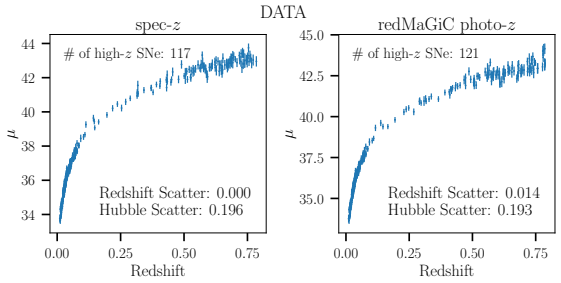

Figure 6: Hubble Diagram as described for Figure 5 but for data.

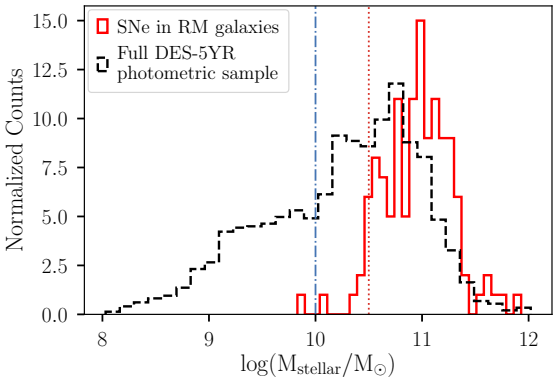

Figure 7: LogMass distribution for the full DES 5YR photometric sample in dashed black and for the subsample of SNe with redMaGiC host galaxies in solid red. The full DES 5YR sample is normalized to the redMaGiC subsample. The red dotted line at logMass of 10.5 indicates the cut made for the simulated host-galaxy library. The blue dash-dotted line indicates the cutoff typically applied to measure the mass step.

3.4 Additional Findings

In the process of this first investigation of using redMaGiC photo-z for SNIa cosmology, we found a number of other interesting results related to host galaxy-SN correlations as well as for using photo-z more broadly. To investigate the claim that the redMaGiC SN subsample is more robust to SN host-galaxy correlations, we consider the mass step (defined in Section 2). However, only 1 in 125 of the SNe has logMass < 10, which is the boundary at which low and high mass galaxies are typically split to measure the mass step. The mass range of the redMaGiC sample is much narrower than the full DES 5YR photometric sample (shown in Figure 7), which indicates that this subsample should be more robust to host-galaxy stellar mass dependencies, where here we use stellar mass as a proxy for other host-galaxy properties.

We also find that when the color-luminosity parameter (β) is floated in the BBC step for the redMaGiC subsample, $\beta = 2.068 \pm 0.210$, which is significantly lower than the $\beta = 3.178 \pm 0.139$ found for the DES 3YR spectroscopic sample. Meldorf et al. (in prep) also find that the redMaGiC subsample has lower reddening ratio (R_V) than the general population of SN host galaxies (~ 1.5 vs. ~ 2.6). This finding supports the claim from [19] that the Hubble scatter correlation with color can be explained by different dust properties in different host galaxies, as it provides a direct link between the low β and associated low R_V predicted for these low dust galaxies.

4 Future Research Plans

There are a number of interesting future prospects related to SNIa cosmology without spectroscopic redshifts that I intend to investigate during my PhD. In the near future, I will begin looking at the formalism and infrastructure required to implement redshift distributions, rather than individual redshifts per event, in the SNIa cosmology pipeline. This is another application to SNe of methods and products used in another cosmological analyses. Another important extension to the analysis detailed in this report is including SN light-curve information for the photometric redshifts. The SALT2 framework in SNANA allows for a simultaneous redshift fit with the light-curve parameters, along with the use of a host-galaxy photo-z prior, but our attempts to implement this resulted in pathologies at high redshift. This was likely due to the fact that only two passbands are not redshifted out of the SALT2 wavelength range, which results in a poorly constrained color and redshift.

I intend to work with other members of the DES SN working group in collaboration with the DES redshift working group to work on finding the optimal unbiased use of photometric redshift information from the SN and host galaxy for SN cosmology analyses. SNIa cosmology with upcoming photometric surveys such as LSST and Roman will require dedicated efforts and methods such as the redMaGiC SN approach to fully make use of the power of these large photometric datasets without the constraints imposed by the limits of spectroscopy.

References

[1] A. G. Riess, A. V. Filippenko, P. Challis, A. Clocchiatti, A. Diercks, P. M. Garnavich, R. L. Gilliland, C. J. Hogan, S. Jha, R. P. Kirshner, B. Leibundgut, M. M. Phillips, D. Reiss, B. P. Schmidt, R. A. Schommer, R. C. Smith, J. Spyromilio, C. Stubbs, N. B. Suntzeff, and J. Tonry. Observational Evidence from Super-

novae for an Accelerating Universe and a Cosmological Constant. , 116:1009–1038, September 1998.

[2] S. Perlmutter, G. Aldering, G. Goldhaber, R. A. Knop, P. Nugent, P. G. Castro, S. Deustua, S. Fabbro, A. Goobar, D. E. Groom, I. M. Hook, A. G. Kim, M. Y. Kim, J. C. Lee, N. J. Nunes, R. Pain, C. R. Pennypacker, R. Quimby, C. Lidman, R. S. Ellis, M. Irwin, R. G. McMahon, P. Ruiz-Lapuente, N. Walton, B. Schaefer, B. J. Boyle, A. V. Filippenko, T. Matheson, A. S. Fruchter, N. Panagia, H. J. M. Newberg, W. J. Couch, and T. S. C. Project. Measurements of Ω and Λ from 42 High-Redshift Supernovae. , 517:565–586, June 1999.

[3] J. Guy, P. Astier, S. Baumont, D. Hardin, R. Pain, N. Regnault, S. Basa, R. G. Carlberg, A. Conley, S. Fabbro, D. Fouchez, I. M. Hook, D. A. Howell, K. Perrett, C. J. Pritchet, J. Rich, M. Sullivan, P. Antilogus, E. Aubourg, G. Bazin, J. Bronder, M. Filiol, N. Palanque-Delabrouille, P. Ripoche, and V. Ruhlmann-Kleider. SALT2: using distant supernovae to improve the use of type Ia supernovae as distance indicators. , 466(1):11–21, April 2007.

[4] J. Guy, M. Sullivan, A. Conley, N. Regnault, P. Astier, C. Balland, S. Basa, R. G. Carlberg, D. Fouchez, D. Hardin, I. M. Hook, D. A. Howell, R. Pain, N. Palanque-Delabrouille, K. M. Perrett, C. J. Pritchet, J. Rich, V. Ruhlmann-Kleider, D. Balam, S. Baumont, R. S. Ellis, S. Fabbro, H. K. Fakhouri, N. Fourmanoit, S. González-Gaitán, M. L. Graham, E. Hsiao, T. Kronborg, C. Lidman, A. M. Mourao, S. Perlmutter, P. Ripoche, N. Suzuki, and E. S. Walker. The Supernova Legacy Survey 3-year sample: Type Ia supernovae photometric distances and cosmological constraints. , 523:A7, November 2010.

[5] R. Tripp. A two-parameter luminosity correction for Type IA supernovae. , 331:815–820, March 1998.

[6] P. Astier, J. Guy, N. Regnault, R. Pain, E. Aubourg, D. Balam, S. Basa, R. G. Carlberg, S. Fabbro, D. Fouchez, I. M. Hook, D. A. Howell, H. Lafoux, J. D. Neill, N. Palanque-Delabrouille, K. Perrett, C. J. Pritchet, J. Rich, M. Sullivan, R. Taillet, G. Aldering, P. Antilogus, V. Arsenijevic, C. Balland, S. Baumont, J. Bronder, H. Courtois, R. S. Ellis, M. Filiol, A. C. Gonçalves, A. Goobar, D. Guide, D. Hardin, V. Lusset, C. Lidman, R. McMahon, M. Mouchet, A. Mourao, S. Perlmutter, P. Ripoche, C. Tao, and N. Walton. The Supernova Legacy Survey: measurement of Ω_M, $\Omega_?$ and w from the first year data set. , 447:31–48, February 2006.

[7] R. Kessler, A. C. Becker, D. Cinabro, J. Vanderplas, J. A. Frieman, J. Marriner, T. M. Davis, B. Dilday, J. Holtzman, S. W. Jha, H. Lampeitl, M. Sako, M. Smith, C. Zheng, R. C. Nichol, B. Bassett, R. Bender, D. L. Depoy, M. Doi, E. Elson, A. V. Filippenko, R. J. Foley, P. M. Garnavich, U. Hopp, Y. Ihara, W. Ketzeback, W. Kollatschny, K. Konishi, J. L. Marshall, R. J. McMillan, G. Miknaitis, T. Morokuma, E. Mörtsell, K. Pan, J. L. Prieto, M. W. Richmond, A. G. Riess, R. Romani, D. P. Schneider, J. Sollerman, N. Takanashi, K. Tokita, K. van der Heyden, J. C. Wheeler, N. Yasuda, and D. York. First-Year Sloan Digital Sky Survey-II Supernova Results: Hubble Diagram and Cosmological Parameters. , 185:32–84, November 2009.

[8] R. Kessler and D. Scolnic. Correcting Type Ia Supernova Distances for Selection Biases and Contamination in Photometrically Identified Samples. , 836:56, February 2017.

[9] T. M. C. Abbott, A. Alarcon, S. Allam, P. Andersen, F. Andrade-Oliveira, J. Annis, J. Asorey, S. Avila, D. Bacon, N. Banik, and et al. Cosmological constraints from multiple probes in the dark energy survey. *Physical Review Letters*, 122(17), May 2019.

[10] C Lidman, B E Tucker, T M Davis, S A Uddin, J Asorey, K Bolejko, D Brout, J Calcino, D Carollo, A Carr, and et al. Ozdes multi-object fibre spectroscopy for the dark energy survey: results and second data release. *Monthly Notices of the Royal Astronomical Society*, 496(1):19–35, May 2020.

[11] C. Frohmaier, M Vincenzi, M. Sullivan, D. Brout, D. Scolnic, R. Kessler, T. M. Davis, C. Lidman, and et al. Lsst sims. in prep.

[12] Masao Sako, Bruce Bassett, Brian Connolly, Benjamin Dilday, Heather Cambell, Joshua A. Frieman, Larry Gladney, Richard Kessler, Hubert Lampeitl, John Marriner, Ramon Miquel, Robert C. Nichol, Donald P. Schneider, Mathew Smith, and Jesper Sollerman. Photometric Type Ia Supernova Candidates from the Three-year SDSS-II SN Survey Data. , 738(2):162, September 2011.

[13] Ryan J. Foley and Kaisey Mandel. Classifying supernovae using only galaxy data. *The Astrophysical Journal*, 778(2):167, Nov 2013.

[14] E. Rozo, E. S. Rykoff, A. Abate, C. Bonnett, M. Crocce, C. Davis, B. Hoyle, B. Leistedt, H. V. Peiris, R. H. Wechsler, and et al. redmagic: selecting luminous red galaxies from the des science verification data. *Monthly Notices of the Royal Astronomical Society*, 461(2):1431–1450, May 2016.

[15] M Vincenzi, M Sullivan, O Graur, D Brout, T M Davis, C Frohmaier, L Galbany, C P Gutiérrez, S R Hinton, R Hounsell, L Kelsey, R Kessler, E Kovacs, S Kuhlmann, J Lasker, C Lidman, A Möller, R C Nichol, M Sako, D Scolnic, M Smith, E Swann, P Wiseman, J Asorey, G F Lewis, R Sharp, B E Tucker, M Aguena, S Allam, S Avila, E Bertin, D Brooks, D L Burke, A Carnero Rosell, M Carrasco Kind, J Carretero, F J Castander, A Choi, M Costanzi, L N da Costa, M E S Pereira, J De Vicente, S Desai, H T Diehl, P Doel, S Everett, I Ferrero, P Fosalba, J Frieman, J García-Bellido, E Gaztanaga, D W Gerdes, D Gruen, R A Gruendl, G Gutierrez, D L Hollowood, K Honscheid, B Hoyle, D J James, K Kuehn, N Kuropatkin, M A G Maia, P Martini, F Menanteau, R Miquel, R Morgan, A Palmese, F Paz-Chinchón, A A Plazas, A K Romer, E Sanchez, V Scarpine, S Serrano, I Sevilla-Noarbe, M Soares-Santos, E Suchyta, G Tarle, D Thomas, C To, T N Varga, A R Walker, R D Wilkinson, and (DES Collaboration). The Dark Energy Survey supernova programme: modelling selection efficiency and observed core-collapse supernova contamination. *Monthly Notices of the Royal Astronomical Society*, 505(2):2819–2839, 05 2021.

[16] Brodie Popovic, Dillon Brout, Richard Kessler, Dan Scolnic, and Lisa Lu. Improved treatment of host-galaxy correlations in cosmological analyses with type ia supernovae. *The Astrophysical Journal*, 913(1):49, May 2021.

[17] A Moller and T de Boissiere. Supernnova: an open-source framework for bayesian, neural network-based supernova classification. *Monthly Notices of the Royal Astronomical Society*, 491(3):4277–4293, Dec 2019.

[18] A. Möller, M. Smith, M. Sako, M. Sullivan, M. Vincenzi, P. Wiseman, P. Armstrong, J. Asorey, D. Brout, D. Carollo, T. M. Davis, C. Frohmaier, L. Galbany, K. Glazebrook, L. Kelsey, R. Kessler, G. F. Lewis, C. Lidman, U. Malik, D. Scolnic, B. E. Tucker, T. M. C. Abbott, M. Aguena, S. Allam, J. Annis, E. Bertin, S. Bocquet, D. Brooks, D. L. Burke, A. Carnero Rosell, M. Carrasco Kind, J. Carretero, F. J. Castander, C. Conselice, M. Costanzi, M. Crocce, L. N. da Costa, J. De Vicente, S. Desai, H. T. Diehl, P. Doel, S. Everett, I. Ferrero, D. A. Finley, B. Flaugher, D. Friedel, J. Frieman, J. García-Bellido, D. W. Gerdes, D. Gruen, R. A. Gruendl, J. Gschwend, G. Gutierrez, K. Herner, S. R. Hinton, D. L. Hollowood, K. Honscheid, D. J. James, K. Kuehn, N. Kuropatkin, O. Lahav, M. March, J. L. Marshall, F. Menanteau, R. Miquel, R. Morgan, A. Palmese, F. Paz-Chinchón, A. Pieres, A. A. Plazas Malagón, A. K. Romer, A. Roodman, E. Sanchez, V. Scarpine, M. Schubnell, S. Serrano, I. Sevilla-Noarbe, E. Suchyta, G. Tarle, D. Thomas, C. To, and T. N. Varga. The Dark Energy Survey 5-year photometrically identified Type Ia Supernovae. *arXiv e-prints*, page arXiv:2201.11142, January 2022.

[19] Dillon Brout and Daniel Scolnic. It's dust: Solving the mysteries of the intrinsic scatter and host-galaxy dependence of standardized type ia supernova brightnesses. *The Astrophysical Journal*, 909(1):26, Mar 2021.